

Full Length Research Paper

Irreversibility analysis of magnetohydrodynamic flow over a stretching sheet with partial slip and convective boundary

Adnan Saeed Butt^{1*}, Asif Ali¹ and Ahmer Mehmood²

¹Department of Mathematics, Quaid-i-Azam University, Islamabad, Pakistan.

²Department of Mathematics (FBAS), International Islamic University, Islamabad, Pakistan.

Accepted 28 March, 2014

The aim of the present article is to study the inherent irreversible effects in magnetohydrodynamic (MHD) flow over a stretching sheet with partial slip and convective boundary. The non-linear partial differential equations governing the flow and heat transfer phenomenon are reduced to a set of non-linear ordinary differential equations with the help of suitable similarity transformations. The transformed equations are then solved analytically with the help of the homotopy analysis method. The expressions for the velocity and the temperature fields are obtained and are utilized to compute the entropy generation number N_s and the Bejan number Be . Both numerical and graphical results are presented and discussed for various physical parameters involved in the problem.

Key words: Boundary layer flow, stretching sheet, partial slip, convective boundary, entropy generation.

INTRODUCTION

The study of boundary layer flow due to stretching surface has gained tremendous attention of researchers during the last few decades due to its wide applications in industrial and manufacturing processes. Some of them are extrusion of a polymer sheet from a dye, cooling of metallic plates, hot rolling, paper production, wire drawing, aerodynamic extrusion of plastic sheets, etc. In the manufacturing of metallic and polymeric sheets, polymers are drawn through a slit die in molten form at significantly higher temperatures. The extrudate is stretched into a sheet which is then solidified through gradual cooling by direct contact with some cooling material such as water. In these cases, the properties of the final product highly depend on the rate of cooling. Crane (1970) initiated the study of boundary layer flow of a viscous fluid due to linearly stretching surface. Gupta and Gupta (1977) analyzed the heat and mass transfer over an isothermal stretching sheet with suction and blowing. Grubka and Bobba (1985) investigated the heat transfer along a linearly stretching sheet by assuming a power law temperature distribution and obtained solution in terms of Kummer's function. Banks (1983) studied the

flow over a stretching surface with power-law velocity variation. Ali (1995) and Elashbeshy (1998) extended the work of Banks for the porous stretched surface. Sriramalu et al. (2001) examined the steady flow and heat transfer of a viscous fluid over a stretching sheet through a porous medium. Andersson (2002) presented the effects of slip on viscous flow over a stretching sheet. Wang (2002) gave the exact solution of the flow due to stretching surface with partial slip. Fang et al. (2009) studied the magnetohydrodynamic viscous flow over a permeable stretching sheet under the effects of slip. Yao et al. (2011) examined the heat transfer phenomenon over a generalized stretching and shrinking sheet with convective boundary surface.

In all the above mentioned papers, a lot of discussion has been made about fluid flow and heat transfer in viscous fluid, yet they have been restricted to only first law analysis from thermodynamical point of view. First

*Corresponding author. E-mail: adnansaeedbutt85@gmail.com.

law of thermodynamics is used to analyze the energy of the system quantitatively. However, from a qualitative point of view, the second law of thermodynamics is an important tool to scrutinize the irreversibility effects due to flow and heat transfer. Thermodynamic irreversibility is closely related to entropy production. Different sources such as heat transfer and viscous dissipation are responsible for the generation of entropy (Bejan, 1996). The pioneer work on entropy generation in flow systems was done by Bejan (1979). He showed that the engineering design of a thermal system could be improved through minimizing the entropy generation.

Since then, many researchers examined the entropy effects in flow and heat transfer problems (San et al., 1987; Sahin, 1998; Yilbas et al., 1999; Hijleh et al., 1998; Mahmud and Fraser, 2003; Odat et al., 2004; Arpaci and Salamet, 1990; Reveillere and Baytas, 2010; Makinde, 2006a, b, 2011, 2012). However, irreversibility effects in flow due to stretchable surfaces were rarely discussed. Tamayol et al. (2010) studied the effects of entropy generation due to heat transfer in a porous medium over a stretching surface with suction and injection. Yazdi et al. (2011) investigated the partial slip effects on entropy generation in magnetohydrodynamic flow over a nonlinear permeable stretching surface. Butt et al. (2012) examined the effects of viscoelasticity on entropy generation in a porous medium over a stretching sheet. The effects of magnetic field on entropy generation over a radially stretching sheet were investigated by Butt et al. (2012) and used analytical and numerical techniques to analyse the problem. Munawar et al. (2013) made thermal analysis of flow over a oscillatory stretching cylinder.

The aim of this study is to investigate the irreversibility effects in a magnetohydrodynamic flow over a stretching surface with partial slip and convective boundary. The effects of viscous dissipation are present in the considered problem.

MATHEMATICAL FORMULATION OF THE PROBLEM

A steady two-dimensional laminar flow of an incompressible viscous fluid over a stretching sheet is considered. The sheet lies in the plane $y = 0$ with the flow being confined to $y > 0$. The coordinate x is being taken along the stretching sheet and y is normal to the surface. Two equal and opposite forces are applied along the x-axis, so that the sheet is stretched, keeping the origin fixed. A uniform transverse magnetic field of strength B_0 is applied parallel to y-axis. It is also assumed that the fluid is electrically conducting and the magnetic Reynolds number is small so that the induced magnetic field is neglected. No electric field is assumed to exist. The temperature of the surface is due to convective heating process which is characterized by a

temperature T_f and a heat transfer coefficient h . Thus, the governing equations for the flow and heat transfer can be written as:

$$\frac{\partial u}{\partial x} + \frac{\partial v}{\partial y} = 0, \tag{1}$$

$$u \frac{\partial u}{\partial x} + v \frac{\partial u}{\partial y} = \nu \frac{\partial^2 u}{\partial y^2} - \frac{\sigma B_0^2 u}{\rho}, \tag{2}$$

$$u \frac{\partial T}{\partial x} + v \frac{\partial T}{\partial y} = \frac{k}{\rho c_p} \frac{\partial^2 T}{\partial y^2} + \frac{\nu}{c_p} \left(\frac{\partial u}{\partial y} \right)^2, \tag{3}$$

The boundary conditions for the velocity and the temperature fields are:

$$\left. \begin{aligned} u = u_w(x) + L \frac{\partial u}{\partial y}, \quad v = 0, \quad -k \frac{\partial T}{\partial y} = h(T_f - T) \quad \text{at } y = 0, \\ u \rightarrow 0, \quad T = T_\infty \quad \text{as } y \rightarrow \infty. \end{aligned} \right\} \tag{4}$$

Where $u_w(x) = ax$, u and v are the x and y components of the velocities respectively, ν is the kinematic viscosity of the fluid, σ is the electrical conductivity of the fluid, B_0 is the applied magnetic field, ρ is the density of the fluid, L is the slip parameter, c_p is the specific heat at constant pressure, k is the thermal conductivity of the fluid, T is the temperature of the fluid, T_f is the wall temperature, T_∞ is the temperature far away from the surface and a is the dimensional constant.

Introducing the similarity transformations, we have the following equation:

$$u = axf'(\eta), \quad v = -\sqrt{av}f(\eta), \quad \theta(\eta) = \frac{T - T_\infty}{T_f - T_\infty}, \quad \eta = \sqrt{\frac{a}{\nu}}y. \tag{5}$$

Using the transformations from equation (5) into equations (1-3), the continuity equation is automatically satisfied and we obtain the following system of non-dimensional equations:

$$f''' + ff'' - f'^2 - Mf' = 0, \tag{6}$$

$$\theta'' + \text{Pr} f \theta' + \text{Pr} Ec f'^2 = 0. \tag{7}$$

The corresponding boundary conditions become:

$$f'(0) = 1 + Kf''(0), \quad f(0) = 0, \quad f(\infty) = 0. \tag{8}$$

$$\theta'(0) = -Bi[1 - \theta(0)], \quad \theta(\infty) = 0. \tag{9}$$

where $M = \frac{\sigma B_0^2}{\rho a}$ is the magnetic field parameter,
 $K = L \sqrt{\frac{a}{\nu}}$ is the non-dimensional slip parameter,
 $\text{Pr} = \frac{\mu c_p}{k}$ is the Prandtl number, $Ec = \frac{a^2 x^2}{c_p (T_f - T_\infty)}$ is
the Eckerd number and $Bi = \frac{h \sqrt{a}}{k}$ is the Biot number.

Entropy generation

Using boundary layer approximation, the local volumetric rate of entropy generation S_G for a viscous fluid in the presence of magnetic field is defined by Bejan (1979) as:

$$S_G = \frac{k}{T_f^2} \left(\frac{\partial T}{\partial y} \right)^2 + \frac{\mu}{T_f} \left(\frac{\partial u}{\partial y} \right)^2 + \frac{\sigma B_0^2}{T_f} u^2. \tag{10}$$

The first term in equation (10) is the irreversibility due to heat transfer, the second term is the entropy generation due to viscous dissipation and the third term is the local entropy generation due to the effect of the magnetic field. In terms of dimensionless variables, the entropy generation has the form:

$$Ns = \frac{S_G}{S_o} = \text{Re}_L \theta'^2 + \text{Re}_L \frac{Br}{\Omega} f'^2 + \text{Re}_L \frac{Br}{\Omega} M f'^2, \tag{11}$$

where $S_o = \frac{k(T_f - T_\infty)^2}{T_f^2 L^2}$ is the characteristic entropy generation rate, $\Omega = \frac{T_f - T_\infty}{T_f}$ is the dimensionless temperature difference and $Br = \text{Pr} Ec$ is the Brinkman

number. Thus dimensionless form of local entropy generation in equation (11) can be expressed as:

$$Ns = N_H + N_f + N_m = N_H + N_F, \tag{12}$$

where N_H is the local entropy generation due to heat transfer, N_f is the local entropy generation due to fluid friction and N_m is the local entropy generation due to magnetic field.

An alternative irreversibility distribution parameter called the Bejan number is defined as follows:

$$Be = \frac{\text{Entropy generation due to heat transfer}}{\text{Total entropy generation}} = \frac{N_H}{Ns}. \tag{13}$$

Clearly, the Bejan number ranges from 0 to 1. When the value of Be is greater than 0.5, the irreversibility due to heat transfer dominates whereas $Be < 0.5$ refers to irreversibility due to viscous dissipation and magnetic field. The contribution of entropy due to heat transfer is equal to that of fluid friction and magnetic field, when $Be = 0.5$.

Solution of the problem

The solution of the nonlinear equations (6) and (7) together with the boundary conditions (8) and (9) are obtained using the homotopy analysis method. This method is proposed by Liao (2003) and in the recent few years, this method has been successfully employed to solve many types of nonlinear problems in Science and Engineering. In view of the boundary data (8) and (9), we choose the following set of initial guesses:

$$f_0(\eta) = \frac{1}{1+K} (1 - e^{-\eta}), \quad \theta_0(\eta) = \frac{Bi}{1+Bi} e^{-\eta}. \tag{14}$$

The linear operators are given as:

$$L_f = \frac{d^3 f}{d\eta^3} - \frac{df}{d\eta}, \quad L_\theta = \frac{d^2 \theta}{d\eta^2} + \frac{d\theta}{d\eta}, \tag{15}$$

All the remaining procedure of the method is renowned and therefore is concealed here for simplicity (Liao, 2003; Ali and Mehmood, 2008, 2010; Hussain et al., 2012). The final solutions obtained by HAM are in the forms of series given by:

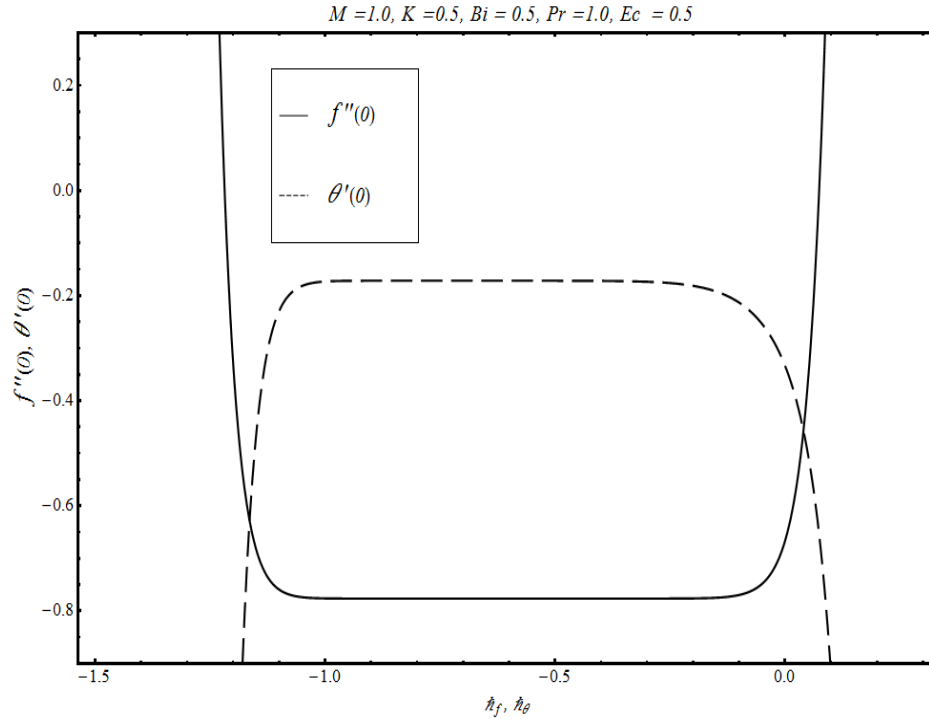


Figure 1. \hbar –curves for 20th order approximation.

Table 1. Convergence of HAM solutions for different order of approximations when $M = 1.0, K = 0.5, Pr = 1.0, Ec = 0.5$ and $h_f = h_\theta = -0.7$

Order of convergence	$-f''(0)$	$-\theta'(0)$
5	0.776570	0.157372
10	0.7765830	0.148219
15	0.7765830	0.147919
20	0.776583	0.147914
25	0.776583	0.147914
30	0.776583	0.147914
35	0.776583	0.147914
40	0.776583	0.147914

called \hbar -curves are drawn in Figure 1 at the 20th order of approximation. It is observed that the suitable ranges

of \hbar_f and \hbar_θ are $-0.2 \leq \hbar_f \leq -1.0$ and $-0.3 \leq \hbar_\theta \leq -0.9$.

Moreover, Table 1 is constructed to present the convergence of series solutions which shows that the series solutions converge at the 25th-order of approximation up to 6 decimal places. Furthermore, the averaged residual errors are calculated by using the formulas:

$$E_{f,m} = \frac{1}{N+1} \sum_{j=0}^N \left[N_f \left(\sum_{i=0}^m f_i(j\Delta\zeta) \right) \right]^2, \quad E_{\theta,m} = \frac{1}{N+1} \sum_{j=0}^N \left[N_\theta \left(\sum_{i=0}^m \theta_i(j\Delta\zeta) \right) \right]^2 \quad (17)$$

$$f(\eta) = f_0(\eta) + \sum_{m=1}^{\infty} f_m(\eta), \quad \theta(\eta) = \theta_0(\eta) + \sum_{m=1}^{\infty} \theta_m(\eta). \quad (16)$$

The convergence of the series solutions $f(\eta)$ and $\theta(\eta)$ strongly depend upon the auxiliary parameters \hbar_f and \hbar_θ . In order to determine the admissible ranges of \hbar_f and \hbar_θ for which the series solutions converge, the so

where $N = 20, \Delta\zeta = 0.05$. Figures 2 and 3 present the averaged residual errors against \hbar_f and \hbar_θ .

RESULTS AND DISCUSSION

Here, the obtained results are compared with a previous study and the variations in the values of skin friction coefficient and Nusselt number are noted for various physical parameters. The velocity and the temperature profile are plotted for the parameters involving in the

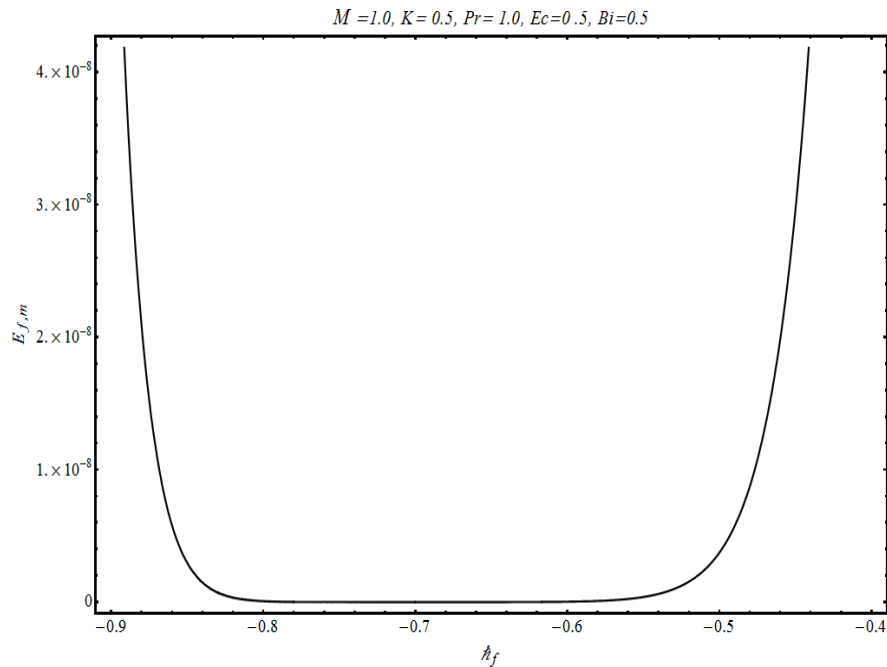


Figure 2. Residual error $E_{m,f}$ for 20th order approximation.

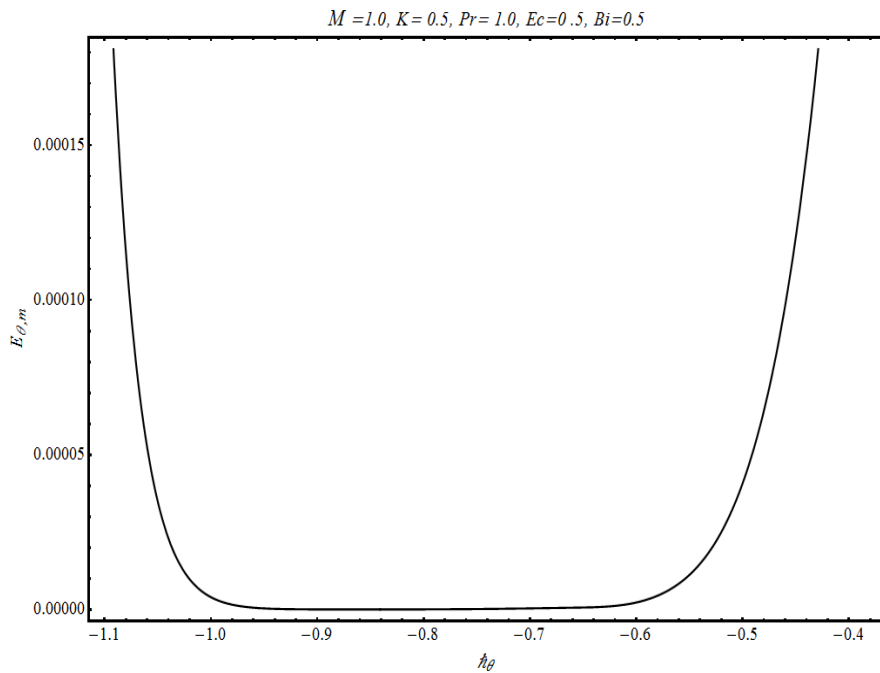


Figure 3. Residual error $E_{m,\theta}$ for 20th order approximation.

problem. Moreover, the effects of these parameters on the local entropy generation Ns and the Bejan number Be are also discussed.

Table 2 gives the comparison of our results of $-f'(0)$ and $-f''(0)$ with those reported by Andersson [8] in the absence of magnetic field parameter. A good agreement

Table 2. Comparison of values of $f'(0)$ and $-f''(0)$ with Andersson [8] when $M = 0.0$.

K	$f'(0)$ [8]	$f'(0)$ Present	$-f''(0)$ [8]	$-f''(0)$ Present
0	1	1	1	1
0.1	0.9128	0.9128	0.8721	0.8721
0.2	0.8447	0.8447	0.7764	0.7764
0.5	0.7044	0.7044	0.5912	0.5912
1.0	0.5698	0.5698	0.4302	0.4302
2.0	0.4320	0.4320	0.2840	0.2840
5.0	0.2758	0.2759	0.1448	0.1448
10.0	0.1876	0.1876	0.0812	0.0812
20.0	0.1242	0.1242	0.0438	0.0438
50.0	0.0702	0.0702	0.0186	0.0186
100	0.0450	0.0449	0.0095	0.0095

Table 3. Values of $f'(0)$ and $-f''(0)$ for different values of M and K .

K	M	$-f''(0)$	$f'(0)$
0.0	1.0	1.41421	1.0
0.1		1.20564	0.879436
0.5		0.776583	0.611709
1.0		0.546602	0.453398
3.0		0.256325	0.231024
5.0		0.168641	0.156796
10.0		0.091250	0.087502
0.5	0	0.591195	0.704402
	0.5	0.698251	0.650875
	1.0	0.776583	0.611709
	1.5	0.838072	0.580964
	2.0	0.888480	0.555760

is observed between the studies which show the accuracy and validity of the homotopy analysis method. Table 3 presents the effects of different values of the slip parameter K and the magnetic field parameter M on $-f''(0)$ and $f'(0)$. It is observed that an increase in the slip parameter causes the values of $-f''(0)$ and $f'(0)$ to decrease. However, opposite behavior is noticed in case of magnetic field parameter. Table 4 depicts the variation of heat transfer at the surface $-\theta'(0)$ for different values of M, K, Bi, Pr and Ec . It is observed that the heat transfer rate at the surface decreases with an increase in the values of

M, K and Ec and increases with Pr and Bi . Figure 4 shows the effects of magnetic field parameter on the velocity profile plotted against the non-dimensional parameter η . It is noticed that an increase in the value of M causes $f'(\eta)$ to decrease. The variation of velocity profile for different values of the slip parameter K is presented in Figure 5. It is noteworthy that an increase in the slip parameter causes $f'(\eta)$ to decrease. Figure 6 shows that the effects of M on temperature profile $\theta(\eta)$ are increasing. The influence of the Prandtl number Pr on $\theta(\eta)$ is presented in Figure 7. A decrease in the temperature profile is noticed with an increase in the values of the Prandtl number. The effects of Eckerd number Ec on temperature profile are illustrated in Figure 8. An increase in thermal boundary layer is observed with increase in the value of Ec . Figure 9 illustrates that an increase in the value of the Biot number Bi causes the thermal boundary layer thickness to increase.

Figures 10-13 depict the influence of different parameters involved in the problem on local entropy generation number N_s . Figure 10 shows the effects of the magnetic field parameter M on the local entropy generation number. It is noteworthy that in the absence of the magnetic field, the entropy generation rate is low. However, the presence of the magnetic field causes more entropy generation in the fluid. Also it is noticed that for a fixed value of M , the entropy generation is maximum near the stretching surface and decreases with η . Figure 11 illustrates that with an increase in the slip parameter K , the friction between the stretching surface and the fluid decreases which ultimately results in less entropy production. The variation in the local entropy generation number N_s for various values of Biot number Bi is presented in Figure 12. There is an increase in N_s with an increase in the value of the Biot number. However, for large values of Bi , these effects are not so prominent. The effects of the group parameter Br/Ω on N_s are significant as it determines the relative importance of viscous effects. It is observed in Figure 13 that the entropy production increases with Br/Ω .

To get an idea of whether the fluid friction and magnetic field irreversibility dominates over the heat transfer or vice versa, the Bejan number Be is introduced. Figure 14 depicts that the irreversibility effects due to fluid friction and magnetic field become dominant near the stretching surface with an increase in the magnetic field parameter M . The situation in reverse in the boundary

Table 4. Values of $-\theta'(0)$ for different values of M , K , Bi , Pr and Ec .

K	M	Bi	Pr	Ec	$-\theta'(0)$
0.0	1.0	0.5	1	0.2	0.187246
0.5					0.185518
1.0					0.171306
3.0					0.126905
5.0					0.100728
0.5	0				0.229466
	0.5				0.205441
	1.0				0.185518
	1.5				0.168671
	2.0				0.154240
0.5	1.0	0.1	1	0.2	0.069102
		0.5			0.185518
		1.0			0.235008
		3.0			0.285843
		5.0			0.298769
0.5	1.0	0.5	0.7	0.2	0.157570
			1.0		0.185518
			2.0		0.238066
			3.0		0.263651
			5.0		0.289006
0.5	1.0	0.5	1	0.1	0.198053
				0.2	0.185518
				0.5	0.147914
				0.8	0.110310
				1.0	0.085241

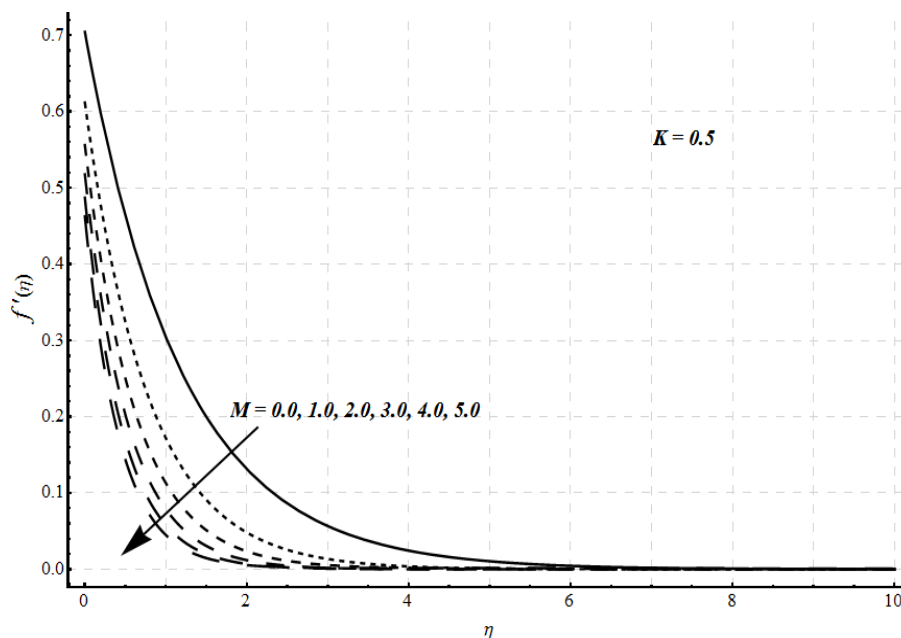


Figure 4. Effects of magnetic field parameter M on velocity profile $f'(\eta)$.

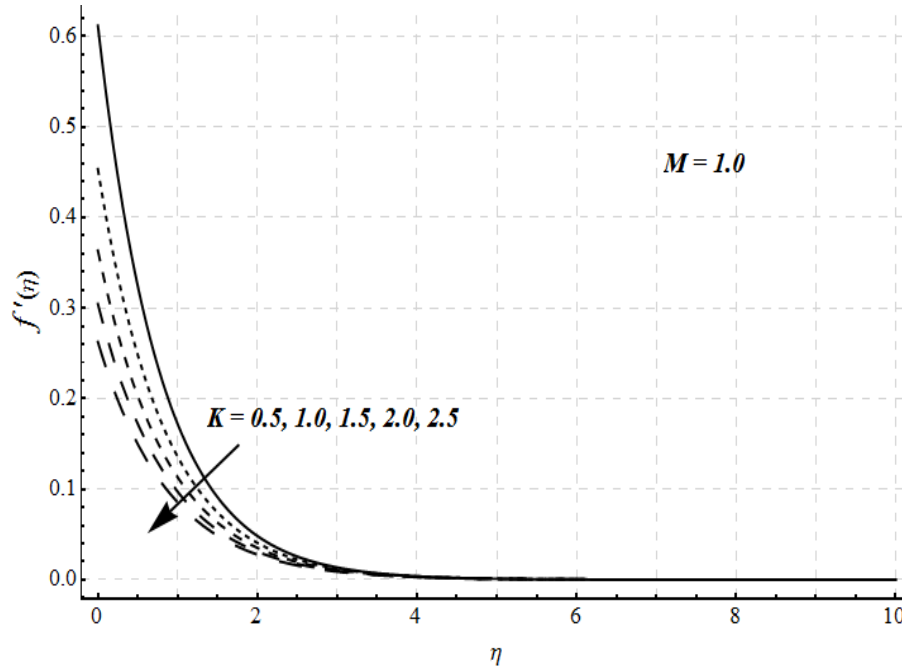


Figure 5. Effects of slip parameter K on velocity profile $f'(\eta)$.

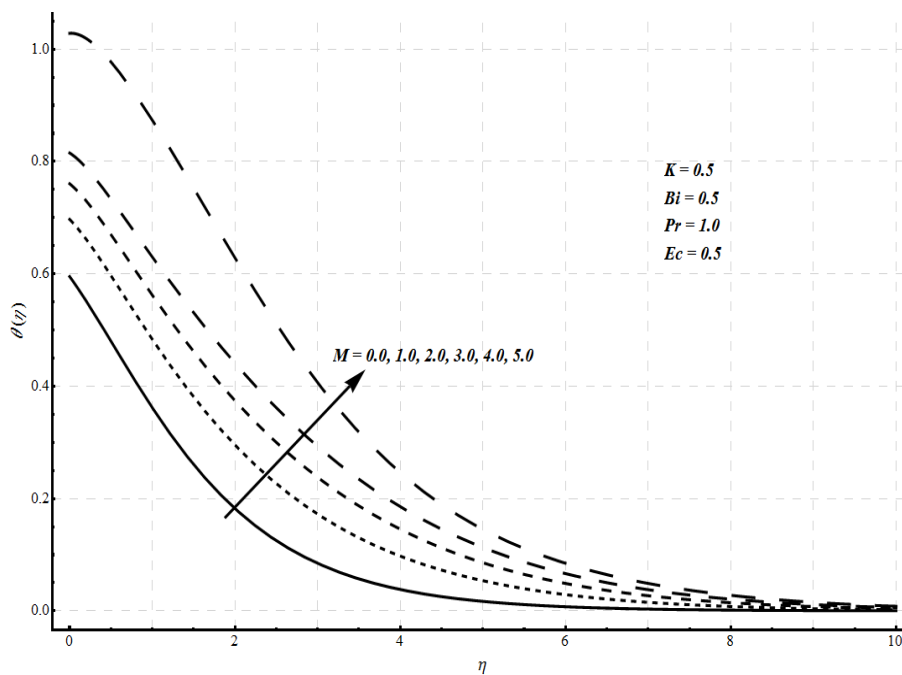


Figure 6. Effects of magnetic field parameter M on temperature profile $\theta(\eta)$.

layer region and the heat transfer irreversibility dominates fully in the mainstream regime. With the increase in slip parameter K , the irreversibility due to fluid friction and magnetic field slightly decreases at the surface. In the

main stream region, the heat transfer irreversibility effects are dominant as shown in Figure 15. Figure 16 illustrates that for a particular value of Biot number, the influence of the fluid friction and magnetic field irreversibility is

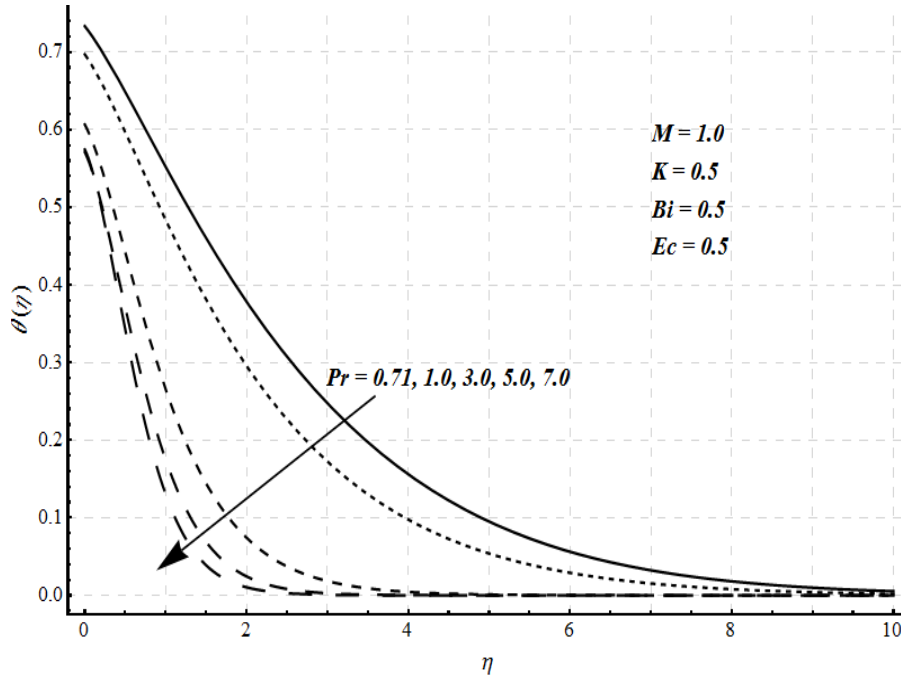


Figure 7. Effects of Prandtl number Pr on temperature profile $\theta(\eta)$.

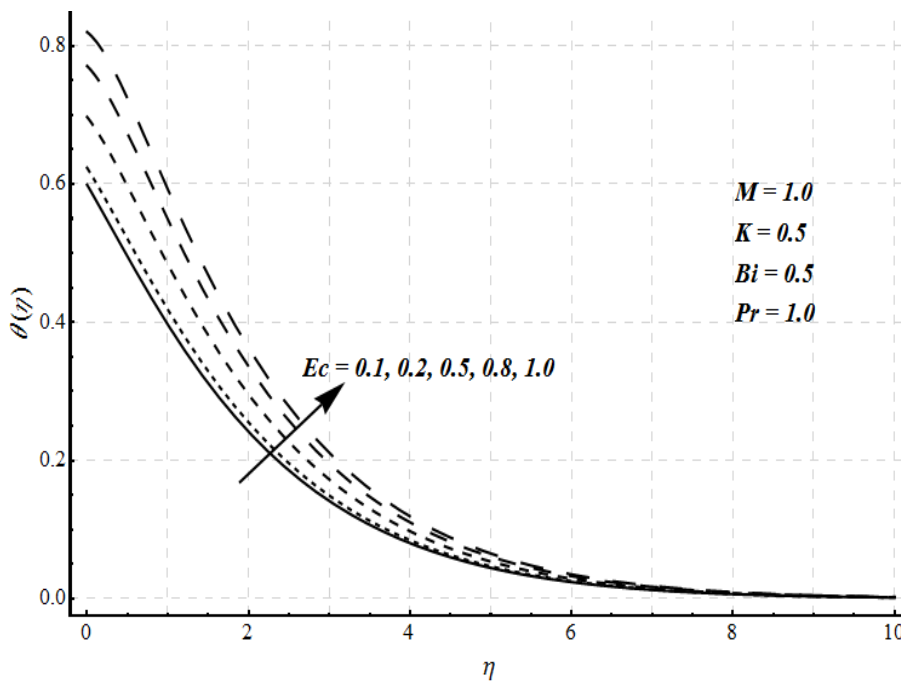


Figure 8. Effects of Eckerd number Ec on temperature profile $\theta(\eta)$.

significant near the surface and in the free stream regime, the heat transfer irreversibility effects are prominent. However, with an increase in the value of Bi ,

the fluid friction and magnetic field irreversibility becomes slightly less near the surface. In case of the group parameter, the fluid friction irreversibility effects become

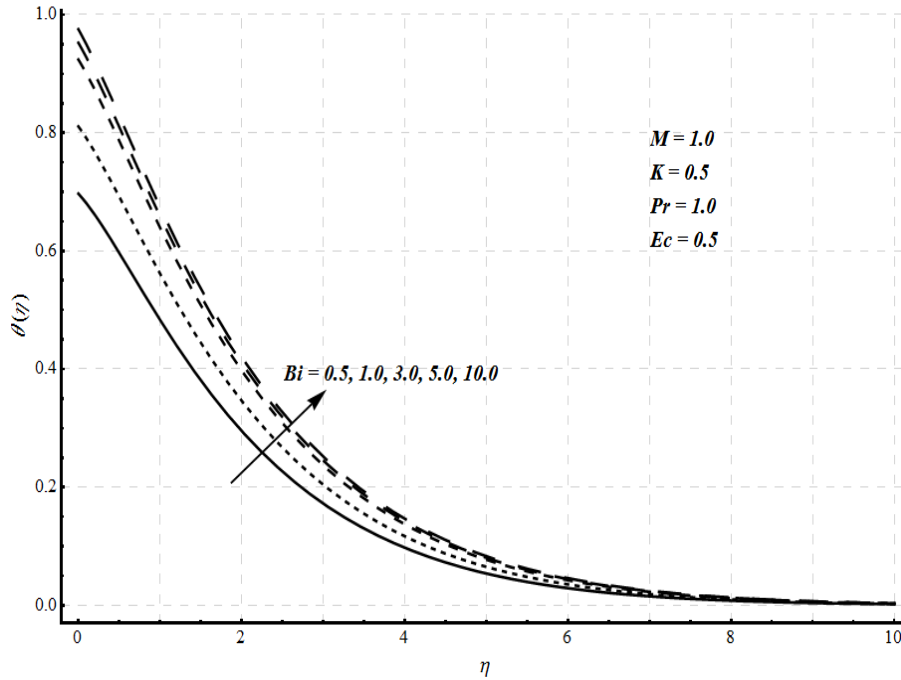


Figure 9. Effects of Biot number Bi on temperature profile $\theta(\eta)$.

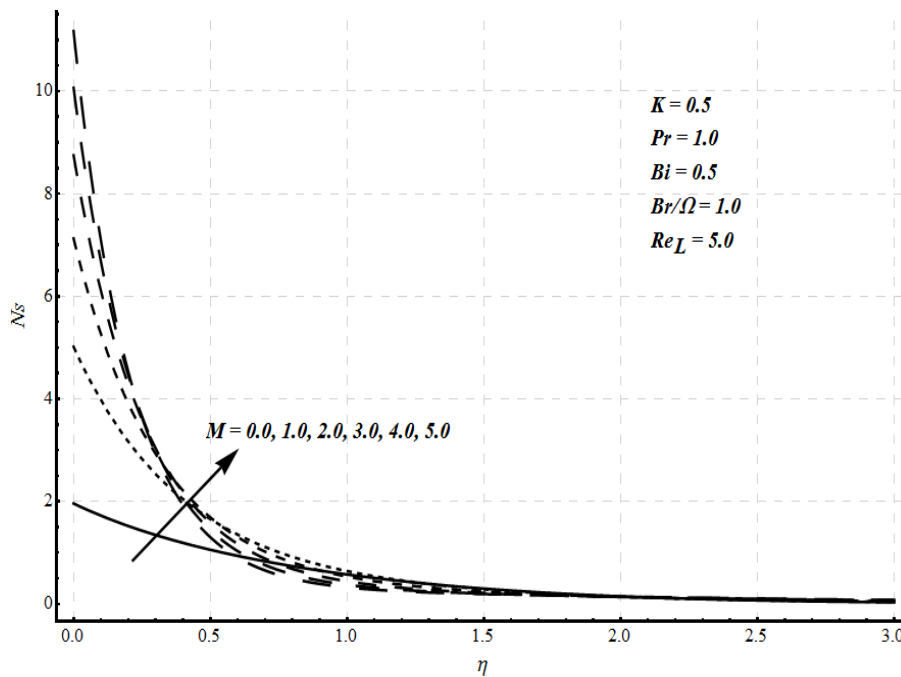


Figure 10. Effects of magnetic field parameter M on local entropy generation Ns .

dominant near the surface with increase in Br/Ω as presented in Figure 17. In the main stream regime, the irreversibility due to heat transfer dominates.

Conclusions

In the present study, the magnetohydrodynamic flow over

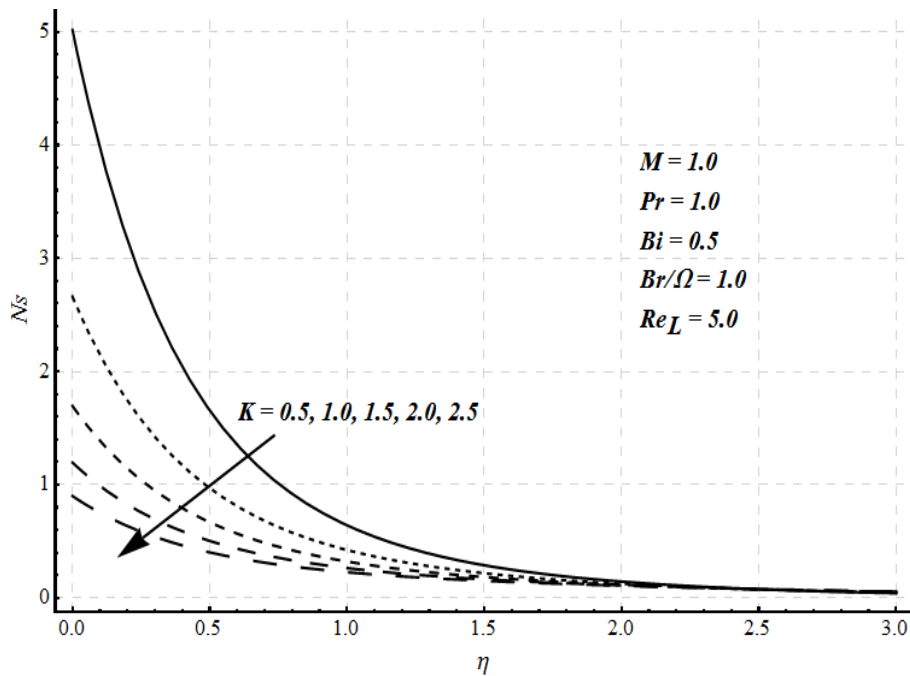


Figure 11. Effects of slip parameter K on local entropy generation Ns .

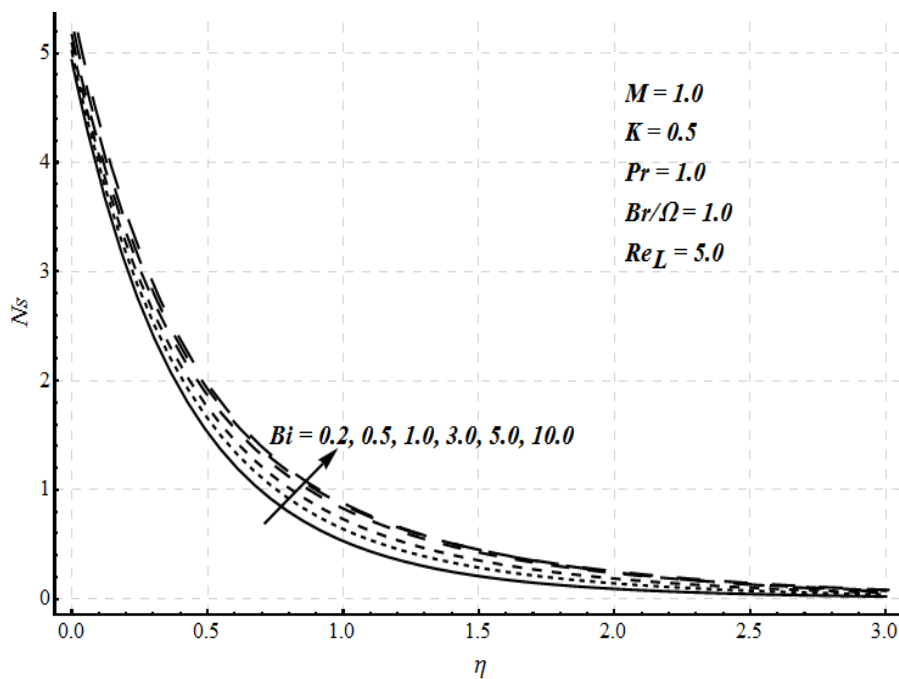


Figure 12. Effects of Biot number Bi on local entropy generation Ns .

a stretching surface with partial slip and convective boundary is considered and the entropy generation effects are studied. The solution is obtained using the Homotopy analysis method and the graphs are presented for different physical parameters. The main observations

of the following study are as follows:

- The velocity profile $f'(\eta)$ decreases with increase in magnetic field parameter M and slip parameter K .

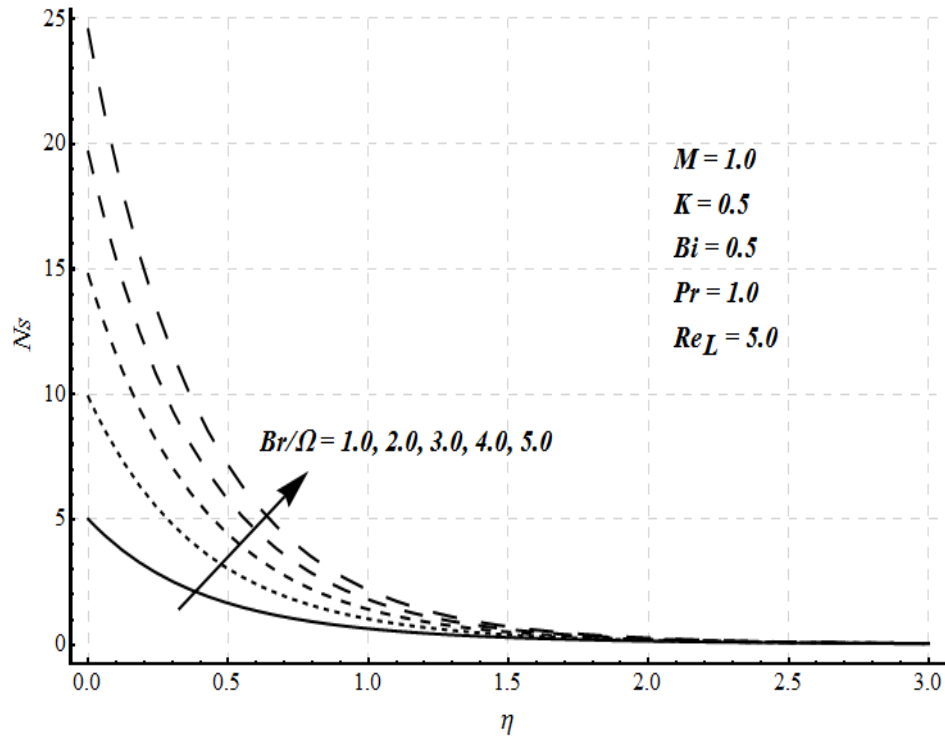


Figure 13. Effects of group parameter Br/Ω on local entropy generation Ns .

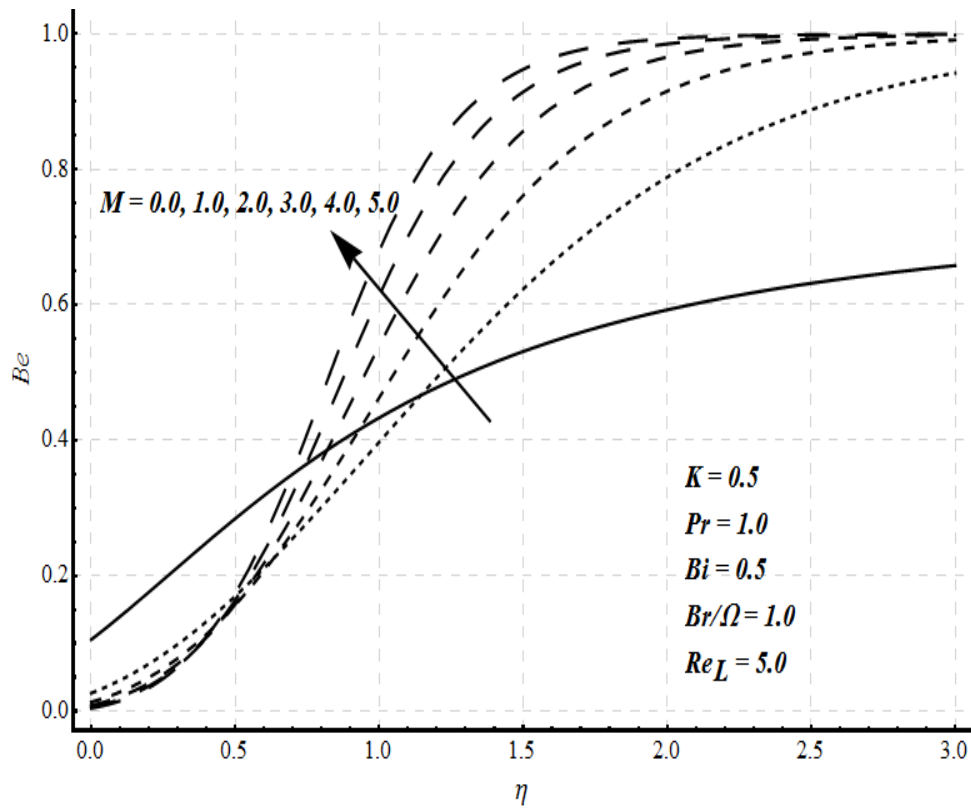


Figure 14. Effects of magnetic field parameter M on Bejan number Be .

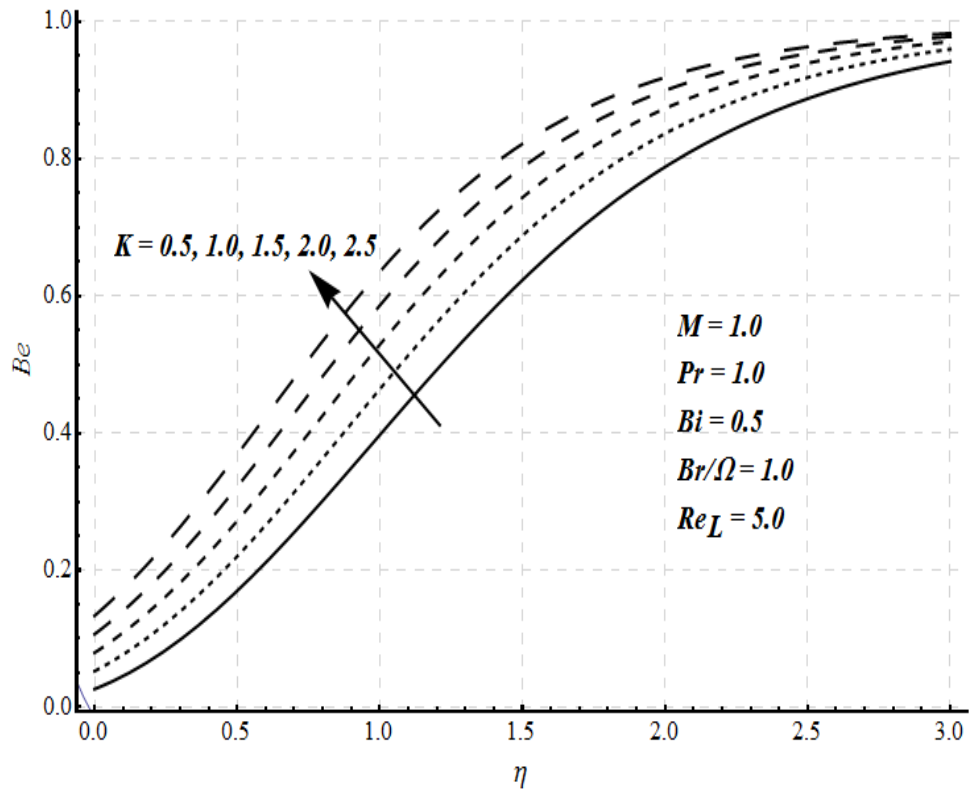


Figure 15. Effects of slip parameter K on Bejan number Be .

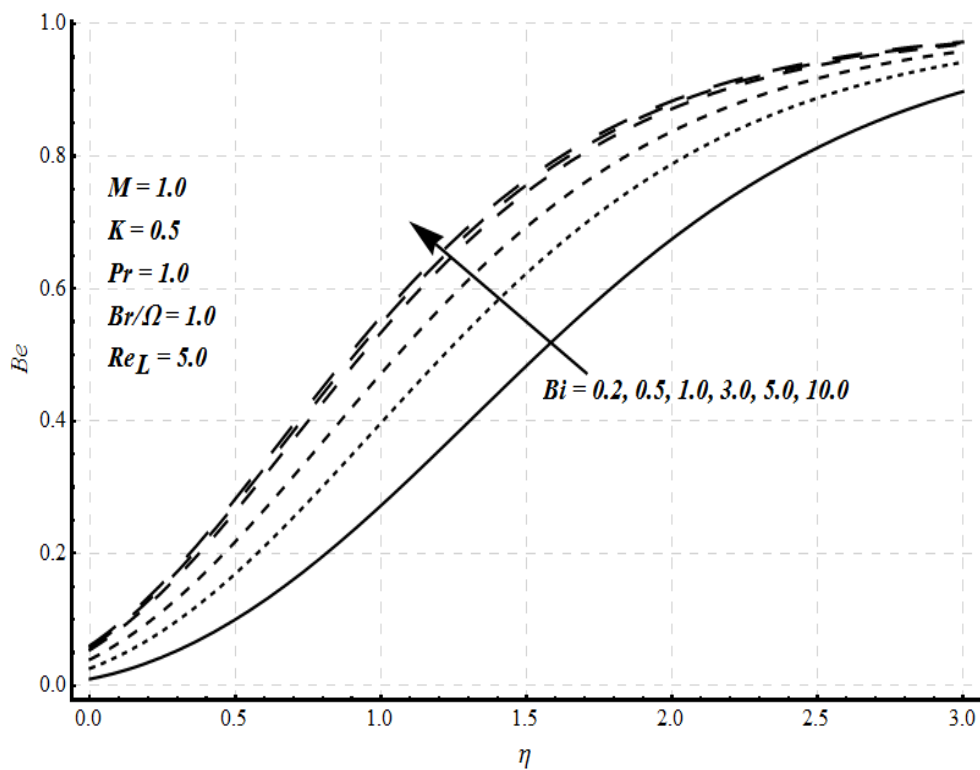


Figure 16. Effects of Biot number Bi on Bejan number Be .

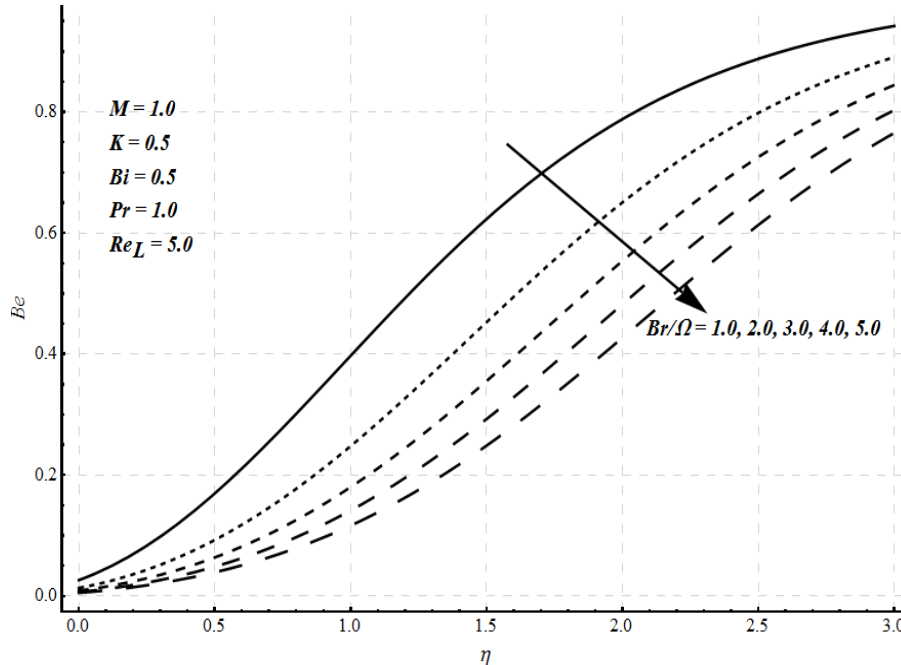


Figure 17. Effects of group parameter Br/Ω on Bejan number Be .

- The temperature profile $\theta(\eta)$ increases with an increase in the values of magnetic field parameter M , Eckerd number Ec and Biot number Bi and decreases with increase in Prandtl number Pr .
- The local entropy generation number increases with magnetic field parameter M , the Biot number Bi and the group parameter Br/Ω , and decreases with the slip parameter K .
- The fluid friction and magnetic field irreversibility dominates near the surface and the heat transfer irreversibility is dominant in the mainstream region.

REFERENCES

- Ali A, Mehmood A (2008). Analytic solution of three-dimensional viscous flow and heat transfer over a stretching flat surface by homotopy analysis method. *ASME-J. Heat Transf.*, 130: 121701-121707.
- Ali A, Mehmood A (2010). Injection flow past a porous plate: Solution to an unsolved problem. *Int. J. Nonlinear Sci. Numerical Simul.*, 11(10): 511-518.
- Ali ME (1995). On thermal boundary layer on a power law stretched surface with suction or injection. *Int. J. Heat Mass Flow*, 16: 280-290.
- Andersson HI (2002). Slip flow past a stretching surface. *Acta Mech.*, 158: 121-125.
- Arpaci VS, Selamet A (1990). Entropy production in boundary layers. *J. Thermophys. Heat Transfer*. 4: 404-407.
- Banks WHH (1983). Similarity solutions of the boundary layer equation for a stretching wall. *J. Mech. Theor. Appl.*, 2: 375 – 392.
- Bejan A (1979). A study of entropy generation in fundamental convective heat transfer. *J. Heat Transf.*, 101: 718-725.
- Bejan A (1996). Entropy Generation Minimization. CRC Press: Boca Raton, FL, USA.
- Butt AS, Ali A (2012). Effects of magnetic field on entropy generation in flow and heat transfer due to radially stretching surface. *Chin. Phys. Lett.*, 30(2): 02704-02708.
- Butt AS, Munawar S, Ali A, Mehmood A (2012). Effect of viscoelasticity on entropy generation in a porous medium over a stretching plate. *World Appl. Sci. J.*, 17(4): 516-523.
- Crane LJ (1970). Flow past a stretching sheet. *Z. Angew. Math. Phys.*, 21: 645-647.
- Elbashaeshy E M A (1998). Heat transfer over a stretching surface with variable heat flux. *J. Physics D: Appl. Phys.*, 31: 1951-1955.
- Fang T, Zhang J, Yao S (2009). Slip MHD flow over a stretching sheet-An exact solution. *Comm. Non. Lin. Sci. Simul.*, 14(11): 3731-3737.
- Grubka J, Bobba KM (1985). Heat transfer characteristics of a continuous stretching surface with variable temperature. *Trans. ASME J. Heat Transfer*, 107: 248 – 250.
- Gupta PS, Gupta AS (1977). Heat and Mass Transfer on a stretching sheet with suction or blowing. *Can. J. of Chem. Eng.*, 55: 744-746.

- Hijleh AKA, Jadallah IN, Nada EA (1998). Entropy generation due to natural convection from a horizontal isothermal cylinder in oil. *Int. Commu. Heat Mass Transfer*, 25: 1135-1143.
- Hussain S, Mehmood A, Ali A (2012). Three-dimensional channel flow of second grade fluid in rotating frame. *Appl. Math. Mech.*, 33(3): 289-302.
- Liao SJ (2003). *Beyond perturbation: Introduction to homotopy analysis method*. Chapman and Hall, CRC Press, Boca Raton.
- Mahmud S, Fraser RA (2003). The second law analysis in fundamental convective heat transfer problems. *Int. J. Therm. Sci.*, 42: 177-186.
- Makinde OD (2006 a). Entropy generation in a liquid film falling along an inclined porous heated plate. *Mech. Research Commu.*, 33(5): 692-698.
- Makinde OD (2006 b). Irreversibility analysis for a gravity driven non-Newtonian liquid film along an inclined isothermal plate. *Phys. Scr.*, 74: 642-645.
- Makinde OD (2011). Second law analysis for variable viscosity hydromagnetic boundary layer flow with thermal radiation and Newtonian heating. *Entropy*, 13: 1446-1464.
- Makinde OD (2012). Entropy analysis for MHD boundary layer flow and heat transfer over a flat plate with a convective surface boundary condition. *Int. J. Exergy*, 10(2): 142-154.
- Mehmood A, Ali A, Shah T (2008). Unsteady boundary-layer viscous flow due to an impulsively started porous plate. *Canadian J. Phys.*, 86: 1079-1082.
- Munawar S, Ali A, Mehmood A (2012). Thermal analysis of the flow over an oscillatory stretching cylinder. *Phys. Scr.*, 86: 065401 doi:10.1088/0031-8949/86/06/065401.
- Munawar S, Mehmood A, Ali A (2011). Unsteady local non-similar boundary-layer flow over a long slim cylinder. *Int. J. Phys. Sci.*, 6(34): 7709 – 7716.
- Munawar S, Mehmood A, Ali A (2012). Time-dependent flow and heat transfer over a stretching cylinder. *Chin. J. Phys.*, 50(5): 828-848.
- Odat MQA, Damseh RA, Nimr MAA (2004). Effect of Magnetic field on entropy generation due to laminar forced convection past a horizontal flat plate. *Entropy*, 4: 293-303.
- Reveillere A, Baytas AC (2010). Minimum entropy generation for laminar boundary layer flow over a permeable plate. *Int. J. Exergy*, 7(2): 164-177.
- Sahin AZ (1998). Second law analysis of laminar viscous flow through a duct subjected to constant wall temperature. *J. Heat Transf.*, 120: 76-83.
- San JY, Laven Z (1987). Entropy generation in convective heat transfer and isothermal mass transfer. *J. Heat Transf.*, 109: 647-652.
- Sriramalu A, Kishan N, Anand RJ (2001). Steady flow and heat transfer of a viscous incompressible fluid flow through porous medium over a stretching sheet. *J. Energy Heat Mass Transfer*, 23: 483-495.
- Tamayol A, Hooman K, Bahrami M (2010). Thermal analysis of flow in a porous medium over a permeable stretching wall. *Transp. Porous Med.*, 85: 661–676.
- Wang CY (2002). Flow due to a stretching boundary with partial slip-an exact solution of the Navier-Stokes equations. *Chem. Eng. Sci.*, 57(17): 3745-3747.
- Yao S, Fang T, Zhong Y (2011). Heat transfer of a generalized stretching/ shrinking wall problem with convective boundary conditions. *Comm. Non. Lin. Sci. Simul.*, 16(2): 752-760.
- Yazdi MH, Abullah S, Hashim I, Zaharim, Sopian K (2011). Entropy generation analysis of the MHD flow over nonlinear permeable stretching sheet with partial slip. *Recent Researches. Energy. Environ.*, 292-297.
- Yilbas BS, Shuja SZ, Budair MO (1999). Second law analysis of swirling flow in a circular duct with restriction. *Int. J. Heat Mass Transf.*, 42: 4027-4041.